Mathematical Modelling of Engineering Problems
Vol. 11, No. 11, November, 2024, pp. 3107-3117
Journal homepage: http://iieta.org/journals/mmep

Numerical Investigation Response of Hollow Steel Cube Under Internal Blast Loading

Geraldy Rivan Pratama[1], Ubaidillah[1*], Eko Prasetya Budiana[1], Ayub Ahmed Janvekar[2], Pramodkumar S. Kataraki[3], Bhre Wangsa Lenggana[4]

[1] Department of Mechanical Engineering, Universitas Sebelas Maret, Surakarta 57126, Indonesia
[2] School of Mechanical Engineering, Vellore Institute of Technology, Chennai 600127, India
[3] School of Mechanical Engineering, REVA University, Bangalore 560064, India
[4] Department of Mechanical Engineering, Universitas Jenderal Soedirman, Purwokerto 53122, Indonesia

Corresponding Author Email: ubaidillah_ft@staff.uns.ac.id

https://doi.org/10.18280/mmep.111122

Received: 8 August 2024
Revised: 29 September 2024
Accepted: 5 October 2024
Available online: 29 November 2024

Keywords:
honeycomb structure, internal blast, numerical simulation, LS-DYNA

ABSTRACT

This study conducts a numerical investigation into the response of a honeycomb sandwich structure cube under internal blast. Three different types of honeycomb core structures with varying numbers of sides were designed to withstand internal blast loads. Numerical simulations were performed using LS-DYNA, applying the same material and volume for the honeycomb core to evaluate the effect of core geometry. Both the honeycomb and steel cube were meshed with shell elements using a default element formulation, with the back plate defined as a fixed support to induce uniform deformation. The Johnson–Cook Material Model was applied for material behavior. Results indicated that as the number of sides of the honeycomb core increased, the front plate experienced less damage, demonstrating improved blast resistance. These findings suggest that optimizing the geometry of honeycomb cores can enhance the energy absorption capacity of structures, making them suitable for protective applications in blast-resistant designs.

1. INTRODUCTION

Hollow cube structures are often found in human creations that existed from ancient times. In an advanced era like today, new risks arise for hollow cube structures that are often used, such as the threat of damage from explosions. In boats, boxcars, as well as truck trailers, hollow cube steel structures are often used. All three have the risk of an explosion threat internally and externally. The source of the explosion can be in the form of a payload explosion, a terrorist attack, or an attack due to a military conflict. The risks that arise require engineers to develop explosion-proof structural designs that are not only safe, but also reliable [1].

Research conducted by Wu et al. [2] found the phenomenon of internal explosions to be more destructive and dangerous than external explosions. Geretto et al. [3] investigated the effect of degree of confinement on the response of a rectangular mild steel plate to blast, it is found that the midpoint deflection increased in direct proportion to the increase in degree of confinement and the damage suffered was four times greater in internal blast. Internal explosions are more destructive because the shock waves generated by the explosion are reflected several times within the structure and will increase at the corners of the structure [2]. When the shock wave spreads to the corners of the structure, the shock waves will meet and converge which will strengthen and have a greater load effect [4]. Research conducted in references [5-7] also shown that internal explosions are more destructive than normal explosions.

Furthermore, in research conducted by Yao et al. [8], conducted research on the hollow steel cube structure on ships using Q235B steel material with TNT (Trinitrotoluene) blast loading and found that increasing the thickness of the material will reduce the displacement received by the material. In this study, the characteristics of the displacement of Q235B steel material against the loading of 40.5 grams of TNT explosion were carried out. In addition, this study also examined the effect of differences in honeycomb structure geometry on the displacement of Q235B steel material due to the loading of 40.5 grams of TNT explosion, as well as how the distribution of Q235B steel material force is at each difference in honeycomb structure geometry due to the loading of 40.5 grams of TNT explosion.

An alternative to adding the thickness of the material is to use a honeycomb sandwich panel structure. The honeycomb sandwich panel structure is often used for its resistance to explosion loading and its ability to absorb energy [9]. The purpose of this study was to determine the effects of differences in the number of sides of honeycomb core geometry in a hollow steel cube under internal explosion. The study will be carried out using numerical simulation software known as LS-DYNA. This study stems from the increasing need for lightweight yet robust structural components in defense, aerospace, and civil engineering applications, where resistance to extreme loading conditions, such as blast impacts, is crucial. Honeycomb sandwich structures are widely

recognized for their excellent strength-to-weight ratio and energy absorption capabilities. However, their performance under internal blast loads, where the force originates from within the structure has not been thoroughly explored.

Internal blasts can cause significant damage, and optimizing the structural response to such events could greatly enhance safety in real-world applications. By investigating the effects of different honeycomb core geometries, this study aims to identify configurations that can improve the blast resistance of structures, reducing material failure and protecting critical components. The findings from this study will contribute valuable insights into the design and development of advanced blast-resistant materials, offering potential solutions for industries requiring enhanced protective measures against high-energy impacts.

2. LITERATURE REVIEW

Recent research has extensively examined the behavior of materials and structures under blast loads. Zhang et al. [10] studied perforated versus non-perforated steel plates, concluding that perforated steel experiences less deformation, highlighting the severity of internal explosions. Yuan et al. [11] further investigated the effect of blast distance on deformation, showing that greater distances result in increased material deformation, with ductility playing a crucial role in preventing rupture [12]. Yao et al. [13] found that increasing plate thickness reduces deflection under blast loads, while Dharmasena et al. [14] demonstrated that honeycomb core structures with square geometries effectively withstand up to 3 kg of TNT.

Stanczak et al. [15] studied variations in the number of honeycomb core cells and found minimal differences in deformation, except in cases with a single cell. Li et al. [16] highlighted the role of kinetic energy in determining panel displacement and damage, showing that greater energy leads to more significant damage.

Research indicates that hollow structures, such as cubes and cylinders, exhibit unique dynamic behaviors under blast conditions due to their geometrical properties. For instance, Matsagar et al. [17] investigated the response of hollow aluminum cylinders, revealing that the geometry significantly influences stress distribution and failure modes. Similar findings were reported by Li et al. [17], who examined the response of thin-walled structures under internal explosions and highlighted the importance of wall thickness and material properties in controlling deformation.

The use of numerical simulations, particularly finite element analysis (FEA), has become a standard approach to evaluate structural responses under blast loading [18, 19]. Studies employing LS-DYNA simulations, such as those by Matsagar [17], have provided insights into the performance of various core structures, demonstrating how different configurations can enhance resistance to dynamic loads. These simulations utilize advanced material models, including the Johnson–Cook Material Model, which accurately captures the material behavior under high strain rates and temperatures, making it an effective tool for blast analysis.

Despite the advancements in understanding the behavior of hollow structures under blast loading, gaps remain in the comparative analysis of different geometric configurations and their influence on structural integrity. This study aims to address these gaps by numerically investigating the response of hollow steel cubes subjected to internal blast loading. By examining various design parameters and employing state-of-the-art numerical techniques, this research seeks to contribute valuable insights into optimizing the design of hollow structures for improved resilience against explosive threats.

Studies focusing on specific materials, such as Q345 and 921A steel, have demonstrated that the thickness of the steel influences the structural response under blast loading. In experiments, it was found that damage modes varied significantly based on the scaled detonation distance and material properties, which aligns with findings from Qin et al. [20], who emphasized the importance of structural integrity in blast scenarios.

Moreover, the concept of damage similarity has been explored through dimensionless numbers to predict damage modes effectively. The introduction of a dimensionless damage number based on dimensional analysis has been proposed in recent research as a promising tool for anticipating damage in stiffened cabin structures under internal blasts. This approach facilitates comparisons across different structural configurations, which can be particularly valuable when considering varying scaled detonation distances.

Notably, the findings indicate that damage modes can exhibit similarities across different materials and thicknesses under specific conditions. For instance, the damage modes of 8 mm Q345 steel structures showed similarities to those of 6 mm 921A steel structures when subjected to internal blast loads. However, discrepancies were noted in larger equivalent explosive blasts, highlighting the complexities involved in predicting structural responses.

Previous studies have conducted by Xu et al. [21] initiated investigations into the response of immersed tunnel structures under blast loading conditions. For instance, a model of the HZMB tunnel was constructed at a scale of 1:5 to conduct explosion tests, revealing significant insights into the structural behavior post-explosion. The results indicated that after an internal explosion from a van-type bomb, the roof subsidence of the tunnel model increased markedly under the same water pressure, illustrating the potential for severe structural compromise. Moreover, the peak overpressure load experienced by the roof reached up to 50 MPa, exhibiting multi-peak characteristics and resulting in noticeable cracking at critical junctions.

To further explore these dynamics, a refined finite element (FE) model based on a verified constitutive model for high strain rate materials was developed. This model facilitated a detailed analysis of blast wave propagation within the tunnel, as well as the dynamic response characteristics and failure modes of the structure. The findings suggested that the ultimate blast resistance of the tunnel model was equivalent to 41.8 kg TNT, with a scaled distance of 0.363 m/kg$^{1/3}$. Additionally, a resonance effect was identified between the middle wall and roof, emphasizing the complex interactions that can occur under explosive loading.

The research also identified critical thresholds for explosion heights, indicating that damage to the roof could be significantly mitigated within the range of 1.06 to 1.25 m. This information could be pivotal for developing traffic standards aimed at ensuring the safe transport of hazardous materials through tunnels. Furthermore, the study categorized four levels of blast damage according to the scaled distance to the tunnel roof, providing a framework for assessing structural integrity under similar conditions.

However, while these studies have provided valuable

insights into material behavior, thickness, and honeycomb core usage, they largely focus on square or standard geometries and external blasts. There is a gap in the literature when it comes to understanding how different honeycomb core geometries, especially those with varying numbers of sides, influence structural integrity under internal blast conditions. This gap is crucial to address, as internal explosions, where the blast originates from within a structure, impose unique challenges due to the confined nature of the energy release.

Thus, this study focuses on filling this gap by investigating how varying honeycomb core geometries impact the response of Q235 steel hollow cubes to internal blasts of 40.5 grams of TNT, providing new insights into blast-resistant design using different honeycomb configurations.

3. METHODOLOGY

3.1 Geometry and material

Structure of this study consisted of 3 parts. The first is the front hollow steel cube, the second one is honeycomb structure, and the last is the back hollow steel cube. These shapes were chosen to represent a progression in the number of sides, allowing us to explore how varying the number of sides impacts the blast resistance of the honeycomb structure. The octagonal geometry, with eight sides, offers a higher degree of symmetry and is expected to distribute stresses more evenly across the structure. The square geometry, with four sides, is a standard shape often used in engineering applications for its simplicity and ease of manufacturing. Lastly, the triangular geometry, with three sides, represents the minimal configuration for a honeycomb structure, making it a baseline comparison to understand how fewer sides affect performance.

Each of these geometries is commonly found in various engineering applications. Square and triangular honeycomb structures are widely used in lightweight materials due to their ease of fabrication and proven performance in energy absorption. The octagonal honeycomb was selected to investigate whether increasing the number of sides beyond the conventional square structure could offer enhanced resistance to internal blasts. By comparing these geometries, we aimed to identify the optimal shape for blast-resistant applications while maintaining practical considerations for manufacturing and structural efficiency. The choice of these geometries was also based on the hypothesis that shapes with more sides would have improved stress distribution and better energy absorption capabilities under internal blast loads. This study aims to explore whether this hypothesis holds true across different geometries and to quantify the differences in performance.

For the front hollow steel cube, a cube with 300 mm side length and 2 mm thickness was used. Then it was connected to a honeycomb core structure with a 51 mm height. And the last one another hollow steel cube was added to cover the honeycomb structure. CONTACT_AUTOMATIC_SURFACE_TO_SURFACE was then used to model the connection between honeycomb and the two hollow steel cubes. Three different types of honeycomb core with different number of sides were used. The three of them were a triangle, square, and octagon honeycomb core. The volume of the honeycomb core was kept at a same value of 2,080,800 mm^3, to keep the same volume amount the thickness of the honeycomb core was then customized with thickness as shown in Table 1. For the blast loading a TNT with 40.5 grams were used and is defined in 0, 0, 0 coordinate using the keyword INITIAL_DETONATION and MAT_HIGH_EXPLOSIVE_BURN. Then to reduce computational costs, the structure modelled is cut down to a half geometry structure as shown in Figure 1.

Table 1. Honeycomb core thickness

	Thickness (m)	Total Honeycomb Volume (mm^3)
Triangle Honeycomb Core	0.001231	2,080,800
Square Honeycomb Core	0.002000	2,080,800
Octagon Honeycomb Core	0.012426	2,080,800

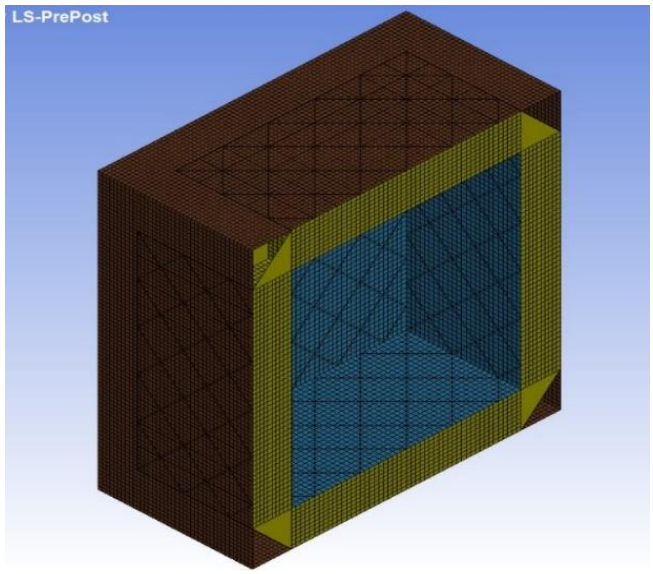

Figure 1. Full view of structure

In this study, the verification technique was carried out using research conducted by Yao et. al. From the research that has been done, a hollow steel cube specimen was used using Q235B steel plate material with a side length of 300 mm of the hollow steel cube. To obtain results that are close to the reference journal, it is necessary to have limiting boundary conditions so that the results do not deviate far from the reference journal and the results of the variation test can be said to be valid. Furthermore, for the type of support on the hollow steel cube, it is not a simply supported or clamped support type, but the hollow steel cube is designed as a single unit without a connection. From the design and support that have been determined, meshing is needed, the design is then meshed using a 5 mm mesh according to the reference journal. After meshing is done, the loading will be carried out, namely the type of free burst water explosion load using an explosion of 40.5 grams of TNT with a time of 1.5×10^{-3} seconds and a time-step of 1×10^{-4} seconds. The results or output taken from the reference journal are the displacement of the center of the side of the hollow steel cube. The results of the tests carried out on the reference journals are shown in Figure 2.

According to Figure 2, the verification simulation data has shown a trend that is close to the data in the reference journal. In the reference journal, the peak displacement occurs at point

0.049 m, while in the verification simulation data, the peak displacement occurs at the same point, namely 0.049 m. With the results obtained in the verification process, the research was continued using the method used in the verification process.

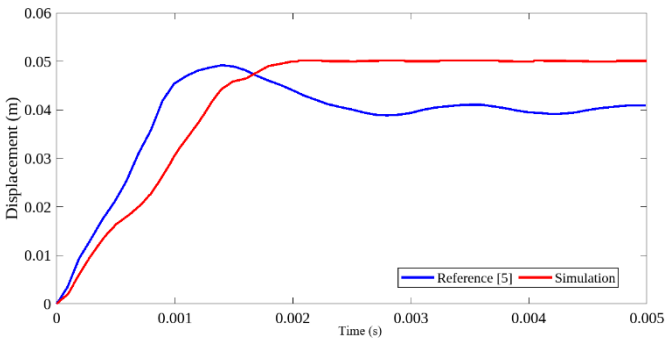

Figure 2. Verification result in previous study

For the triangle honeycomb core, a triangle with dimensions of 0.03, 0.03, and 0.04 m side length as shown in Figure 3 was used.

And for the last one, octagon honeycomb core. An octagon with dimensions of 0.01 m side length as shown in Figure 4 was used.

For the square honeycomb core, a square with dimensions of 0.03 m side length as shown in Figure 5 was used.

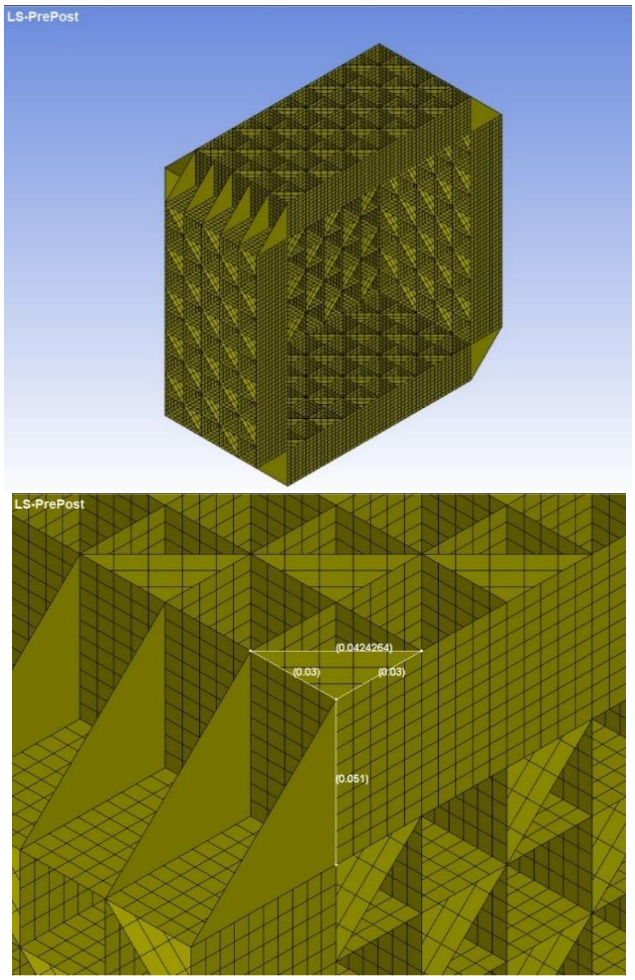

Figure 3. Triangle honeycomb core

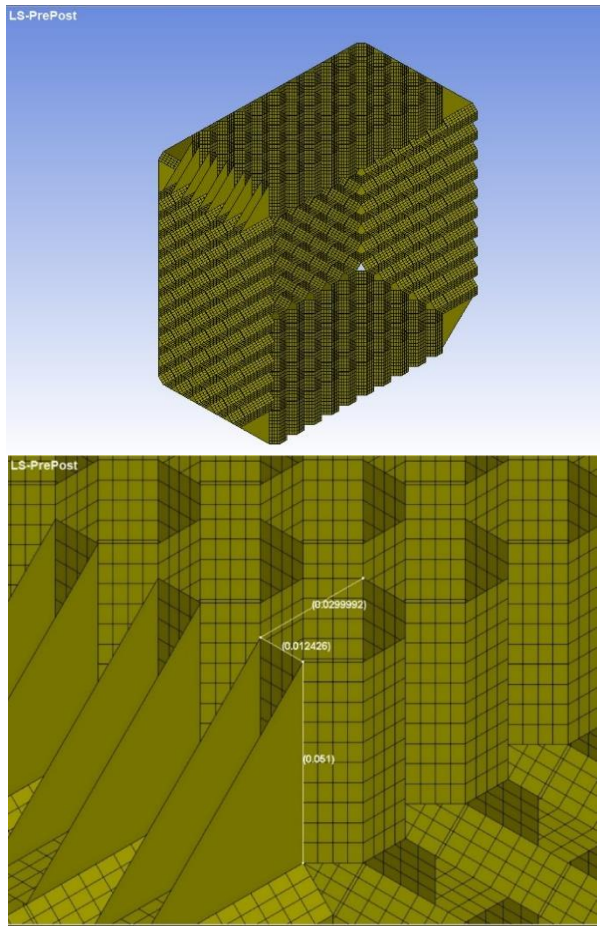

Figure 4. Octagon honeycomb core

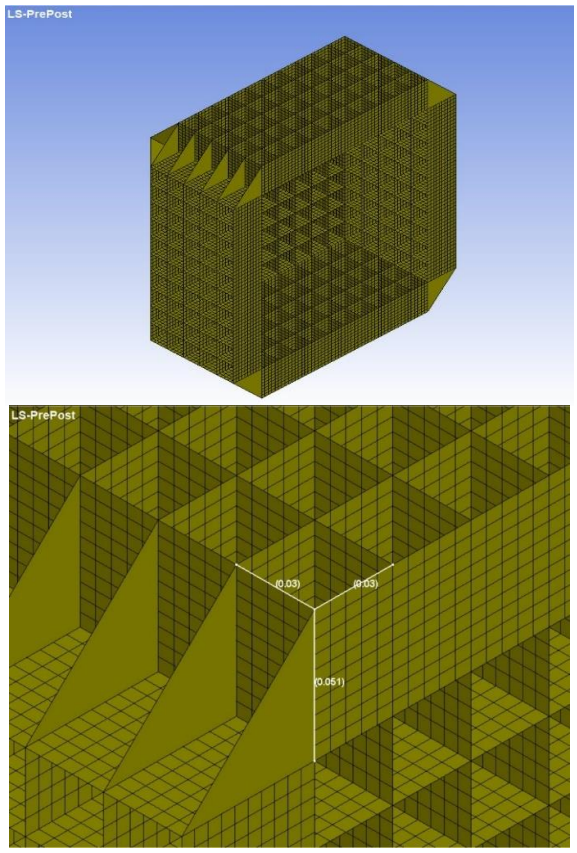

Figure 5. Square honeycomb core

3.2 Johnson-Cook Material Model and Gruneisen EOS

The Johnson-Cook Material Model parameters used in this study were selected based on material properties provided in existing literature and validated data specific to the steel material used in the honeycomb sandwich structure. The parameters were chosen to closely match the mechanical behavior of the materials under high strain rates and temperature conditions, which are typical in blast loading scenarios.

Assumptions made during parameter selection include the material's isotropic behavior and homogeneity, which are common in numerical simulations but may not fully capture real-world material imperfections or anisotropies. Furthermore, the thermal effects in this study were assumed to be minimal due to the relatively short duration of the blast event, allowing us to focus primarily on the strain and strain rate effects. These assumptions are discussed in the limitations section, where suggestions for more detailed future studies are provided.

3.2.1 Johnson-Cook Material Model

The Johnson-Cook Material Model is a model used to model the characteristics of various materials that experience high levels of deformation. Typical applications include use to model explosive metal forming, ballistic penetration, and impact [16]. Johnson and Cook express the stress flow as follows in the Eq. (1) [16, 22].

$$\sigma_y = \left(A + B\varepsilon^{-p^n}\right)(1 + cln\dot{\varepsilon}^*)[1 - \left(\frac{T-T_0}{T_{melt}-T_0}\right)^m] \quad (1)$$

where, A, B, C, n, and m are material parameters, ε^p is the effective plastic strain, $\dot{\varepsilon}^*$ is $\frac{\dot{\varepsilon}^{-p}}{\dot{\varepsilon}_0}$ or the effective plastic strain for $\dot{\varepsilon}_0$ in units one per time unit, T is the actual temperature, T_{melt} is the melting temperature, and T_0 is the transition temperature.

Furthermore, the Johnson-Cook Material Model requires the strain rate, temperature at equivalent failure, and the effect of stress triaxiality as can be seen in the Eq. (2).

$$\varepsilon^f = \left[D_1 + D_2 exp\left(D_3 \frac{\sigma_m}{\bar{\sigma}}\right)\right][1 + D_4 ln\varepsilon^*][1 + D_5\left(\frac{T-T_0}{T_{melt}-T_0}\right)^m] \quad (2)$$

where, D_1-D_5 are material parameters that have been obtained from various processes, $\frac{\sigma_m}{\sigma}$ is the triaxiality stress ratio, σ_m is the average stress, and $\bar{\sigma}$ is the equivalent von Mises stress.

3.2.2 Gruneisen equation of state

The Gruneisen equation is an equation used to determine the stress in a shock-compressed solid. The Gruneisen equation is expressed by the following equation:

$$P = \frac{\rho_0 C^2 \mu[1+\left(1-\frac{\gamma_0}{2}\right)\mu - \frac{a}{2}\mu^2]}{[1-(S_1-1)\mu - S_2\frac{\mu^2}{\mu+1} - S_3\frac{\mu^3}{(\mu+1)^2}]^2} + (\gamma_0 + \alpha\mu)E \quad (3)$$

where, E is the initial internal energy per volume, C is the section of the Hugoniot curve, S_1, S_2, and S_3 are the coefficients of the slope of the Hugoniot curve, γ_0 is the Gruneisen gamma, a is the first-order volume correction with respect to γ_0. From the equation, the constants C, S_1, S_2, S_3, γ_0, and a will be obtained which will be used to model the dynamic characteristics of the model [16].

3.2.3 Johnson-Cook Material Model and Gruneisen equation of state parameters

Johnson-Cook Material Model and Gruneisen equation of State was used to model the dynamic behavior of the hollow cube and honeycomb structure. The parameter of Johnson-Cook Material Model and Gruneisen equation of State are as listed in Table 2 [8, 23-26].

Table 2. Parameters of Johnson-Cook Material Model and Gruneisen equation of state for Q235B Steel

JC Material Model	ρ (kg/m²)	E (GPa)	G (GPA)	Poisson's Ratio	A (GPa)	B (GPa)
	7800	210	80.8	0.3	370	438
	n	c	m			
	0.60	0.01	0.669			
Gruneisen EOS	C (m/s)	S1	S2	S3	γ_0	a
	4569	1.49	0	0	2.17	0.46

4. RESULT

4.1 Result displacement

The front centre plate result displacement data obtained is as shown in Figure 6. According to Figure 6, the peak displacement data for the triangular honeycomb variation is 0.0093 m, then the peak displacement for the square honeycomb is 0.0035 m, and the peak displacement for the octagon honeycomb is 0.0028 m. From these data, the greater the number of sides in the honeycomb core geometry, the lower the peak displacement will be.

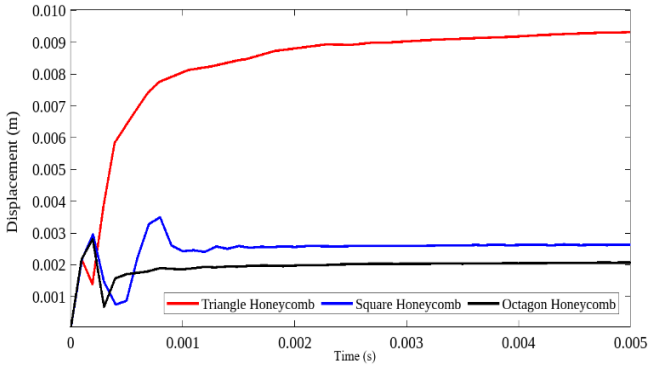

Figure 6. Result displacement

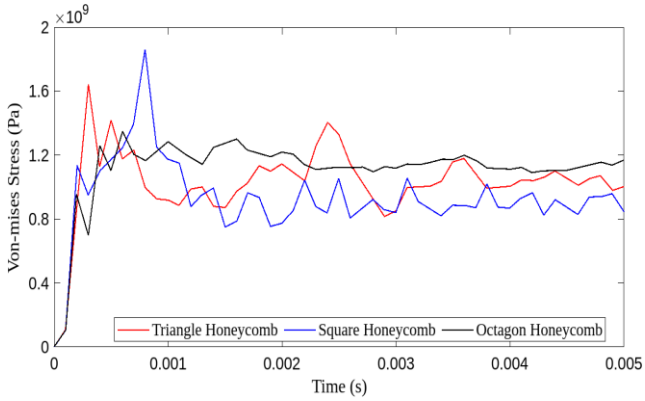

Figure 7. Von-mises stress

4.2 Von-mises stress

After the displacement graph is obtained, the Von-mises stress graph data will be retrieved from the simulation that has been carried out. The Von-mises stress graph obtained is as follows.

According to Figure 7, after 0.001 seconds the graph volatility of each variation decreased with the difference between the peaks and valleys of the graph in the triangle, square, and octagon honeycomb variations, respectively, being 5.889E+08, 4.250E+08, 2.100E+08 Pa as can be seen in Table 3.

Table 3. Von-mises stress volatility

	Triangle Honeycomb	Square Honeycomb	Octagon Honeycomb
Max (Pa)	1,405 E+09	1,175 E+09	1,301 E+09
Min (Pa)	8,161 E+08	7,504 E+08	1,091 E+09
Difference (Pa)	5,889 E+08	4,250 E+08	2,100 E+08

The largest difference occurs in the triangular honeycomb variation and the smallest difference occurs in the octagon honeycomb. In the triangular honeycomb with the largest stress difference after 0.001 seconds, the displacement of the triangular honeycomb variation has increased which is still quite large when compared to the other two variations, namely an increase from 0.008 up to 0.009 m. While the other two variations of honeycomb geometry with a smaller difference did not experience a large increase in the displacement experienced.

4.3 Kinetic energy

Furthermore, the research will compare the results of the kinetic energy received by each variation. The kinetic energy data obtained is from the whole honeycomb core structure and can be seen in Figure 8.

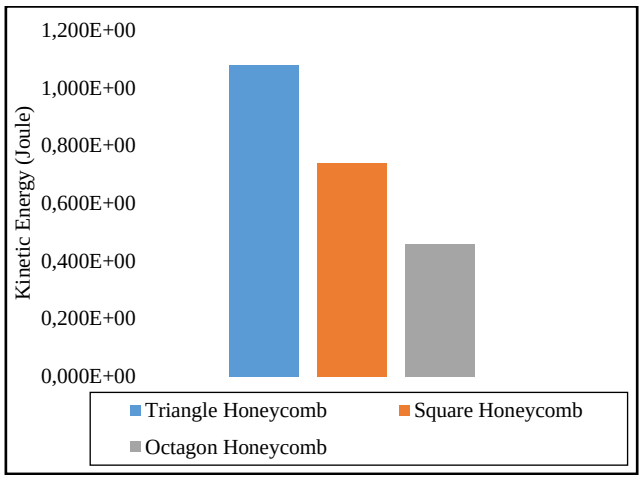

Figure 8. Kinetic energy

According to Figure 8, the variations of the honeycomb core that receive the greatest to the smallest kinetic energy are the triangular, square, and octagon honeycomb core variations, respectively. The triangular honeycomb gets the most kinetic energy with an energy value of 1.080E+03 Joule, then the square honeycomb with the second largest kinetic energy value gets a kinetic energy value of 7.394E+02, and the octagonal honeycomb has the lowest value with a value of 4.596E +02 Joules. The kinetic energy obtained from each variation shows results that are directly proportional to the displacement experienced or in other words the greater the kinetic energy value received, the greater the displacement value obtained. The kinetic energy results obtained is in accordance with the study conducted by Matsagar [17] which stated that kinetic energy received is proportional to the displacement.

4.4 Deformation results

After the displacement, von-Mises stress, and kinetic energy data are known, then the deformation results of the triangular, square and octagon honeycomb core geometries will be displayed. Then, from the LS-Dyna program, the results of the deformation with pressure, displacement, and von-mises stress fringes will be displayed. Firstly, the pressure deformation results from each variation of the honeycomb core geometry will be displayed which can be seen in Figures 9 to 11.

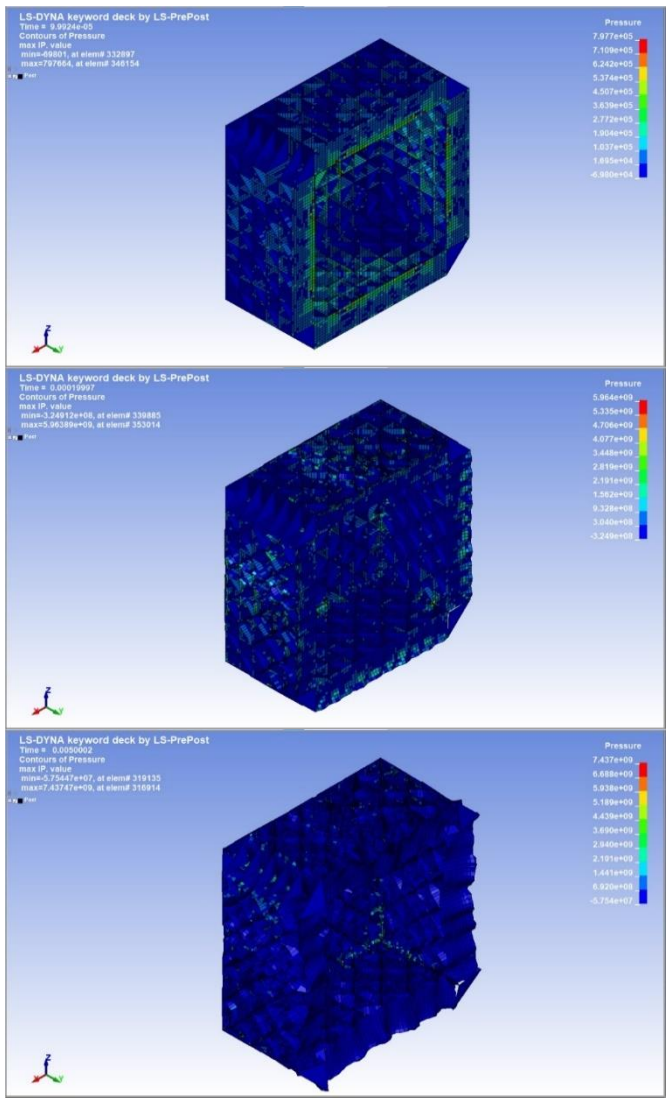

Figure 9. Triangle honeycomb core pressure (first, second, and last phase)

The first phase of each honeycomb core variation shows that the triangular honeycomb has the highest maximum pressure value compared to the other two variations with a

pressure value of 7,977 E+05 Pa. Furthermore, in the second phase, the octagon honeycomb core variation shows the minimum red color contour when compared to the other two variations. And finally, in the last phase, the octagon honeycomb core variation was found with the smallest maximum pressure value when compared to the other two variations.

Next is a displacement contour image in the x, y, and z directions experienced by each variation of the honeycomb core. The maximum value is indicated by the red contour color on the fringe and the minimum value by the blue contour color. The results that have been obtained can be seen in Figures 12 to 14.

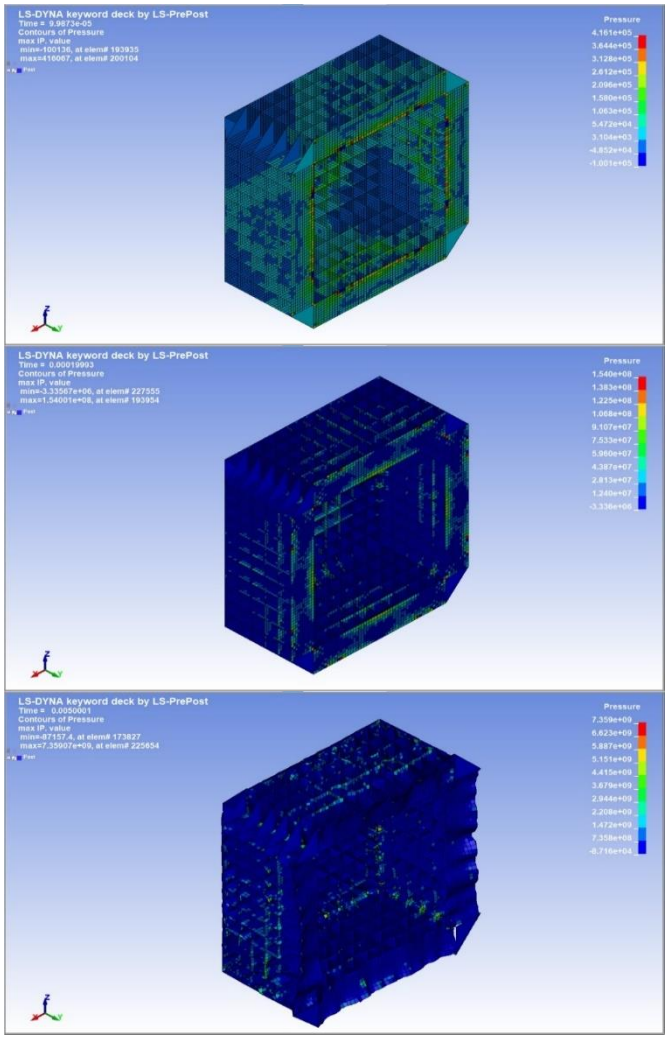

Figure 10. Square honeycomb core pressure (first, second, and last phase)

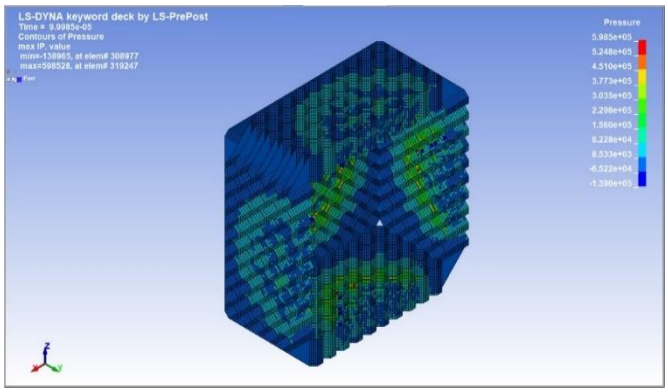

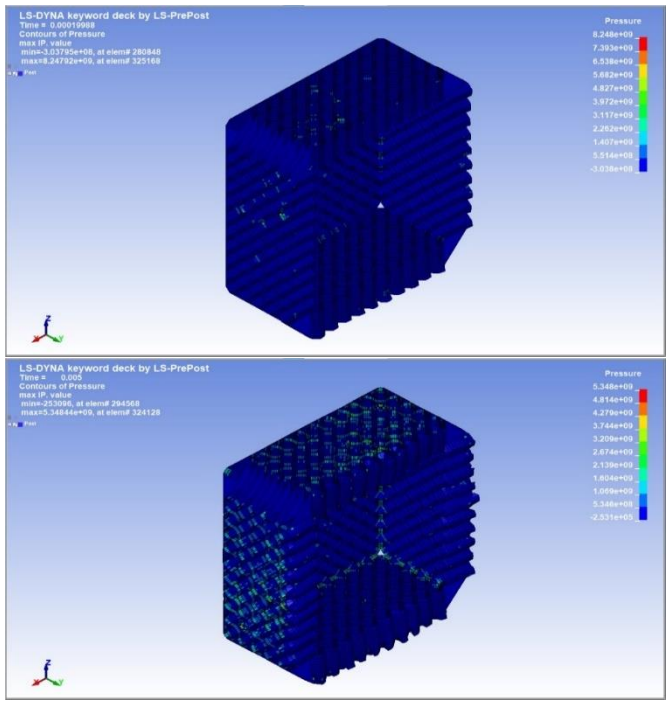

Figure 11. Octagon honeycomb core pressure (first, second, and last phase)

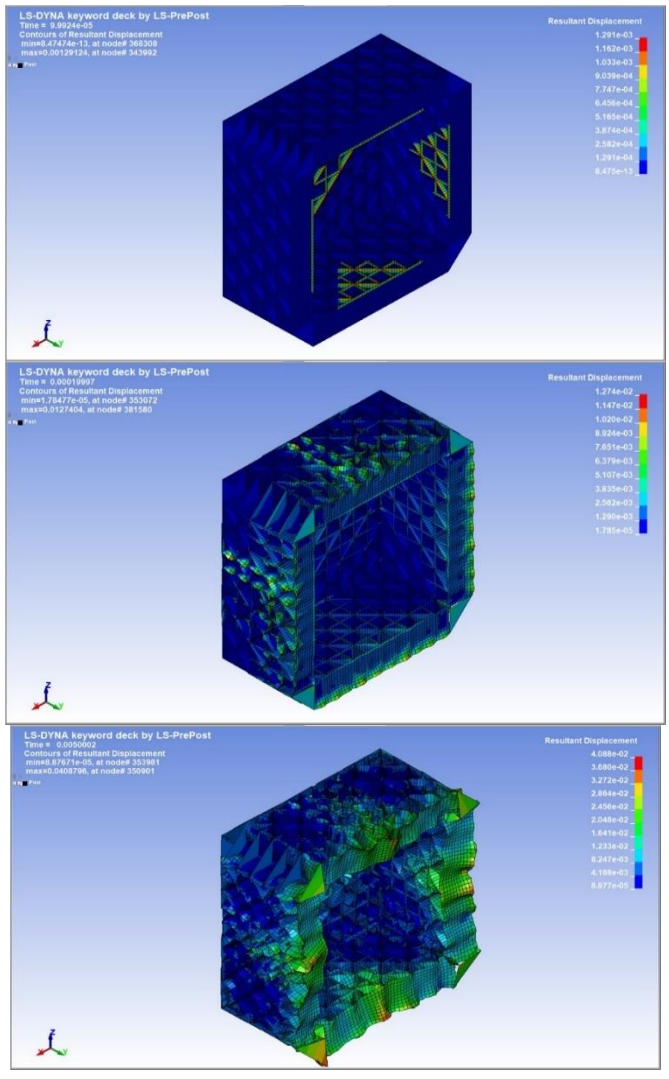

Figure 12. Triangle honeycomb core displacement (first, second, and last phase)

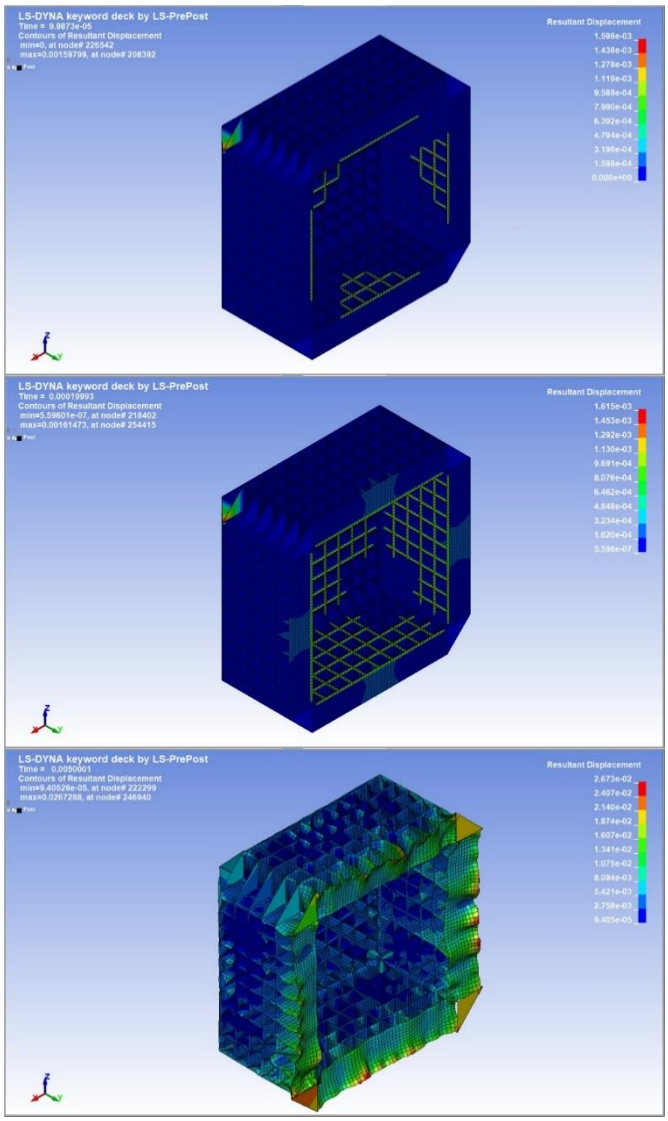

Figure 13. Square honeycomb core displacement (first, second, and last phase)

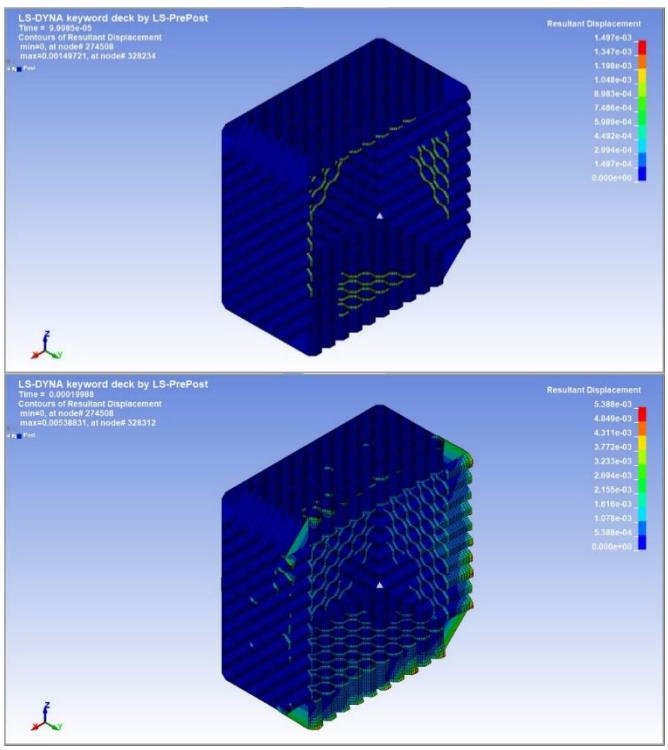

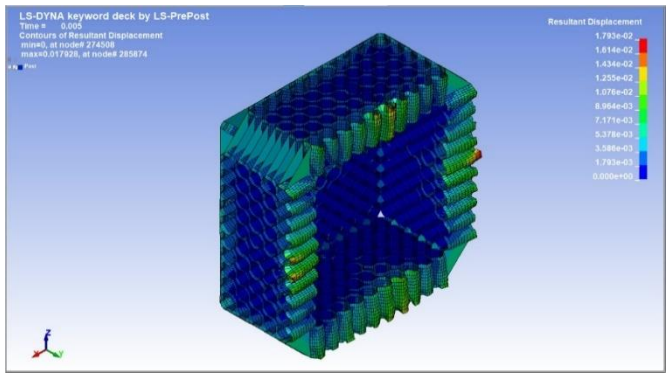

Figure 14. Octagon honeycomb core displacement (first, second, and last phase)

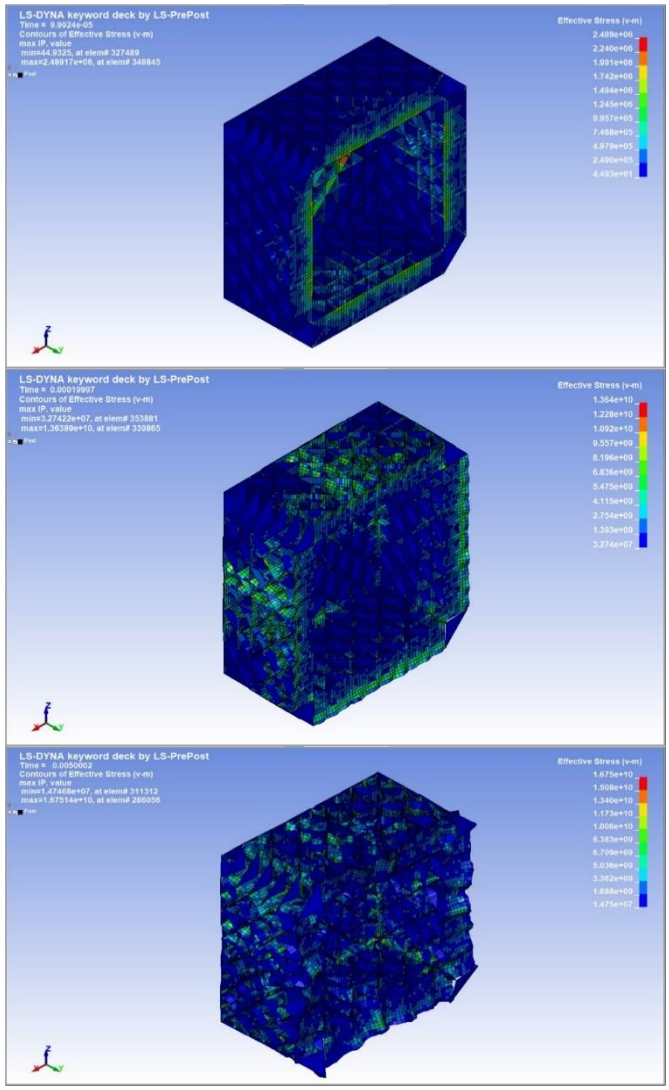

Figure 15. Triangle honeycomb core von-mises stress (first, second, and last phase)

Based on the color contour of the displacement during the first phase in each variation, it can be seen that in the initial conditions the affected part is the inner part of the honeycomb core, except for the square honeycomb core, there is an outer part connecting the side being affected. In the second phase the highest maximum value was found in the triangular honeycomb with a displacement value of 1,274 E-02 m. Furthermore, in the last phase it can be seen that the octagon honeycomb variation was found with the least red color

contour which is in accordance with the data in Figure 6.

The third is the result of the von-mises stress experienced by each variation of the honeycomb core. The color contour characteristics at the fringe level are the same as the color contour characteristics at pressure and the displacement with the red contour is the maximum von-mises stress value experienced. The results of the von-mises stress obtained can be seen in Figures 15 to 17.

In Figures 15 to 17, the behavior of the stress can only be seen under certain circumstances. The red contour of the figure shows the maximum stress value, so this shows that the red part is the part that receives the greatest stress. When viewed from the three variations, it can be seen that the octagon honeycomb core variation has the least amount of red contours compared to the other two honeycomb core variations.

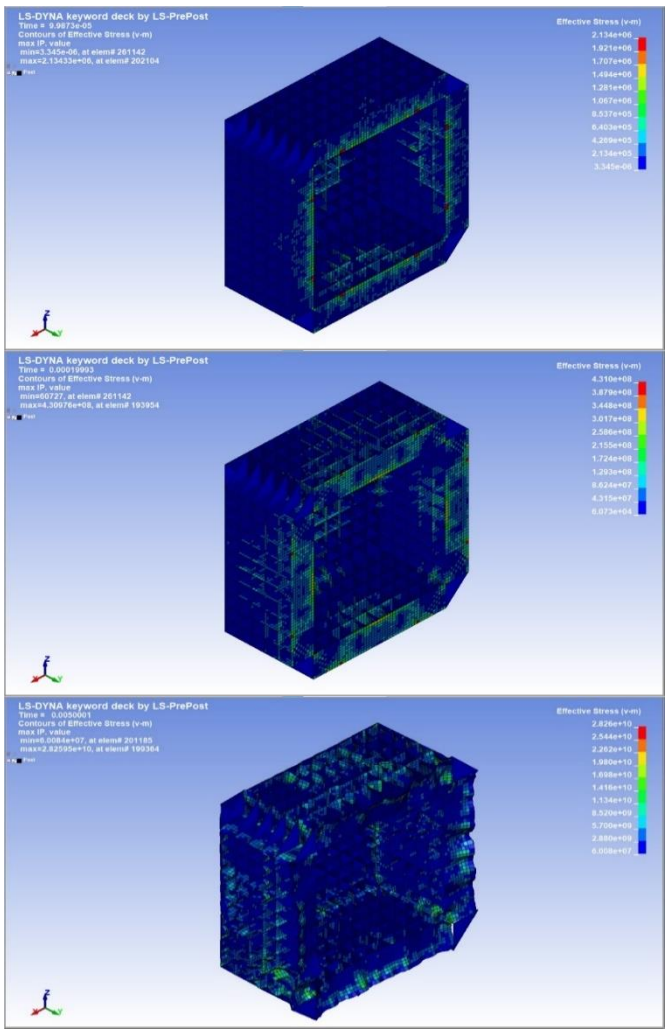

Figure 16. Square honeycomb core von-mises stress (first, second, and last phase)

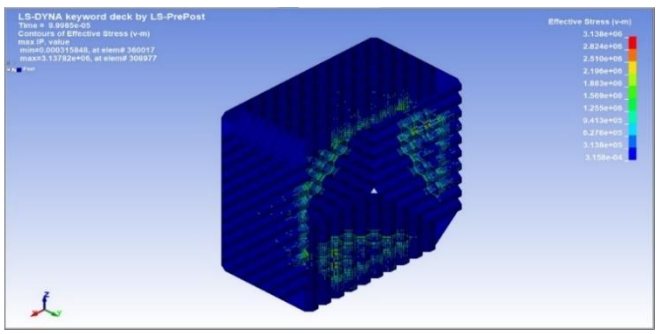

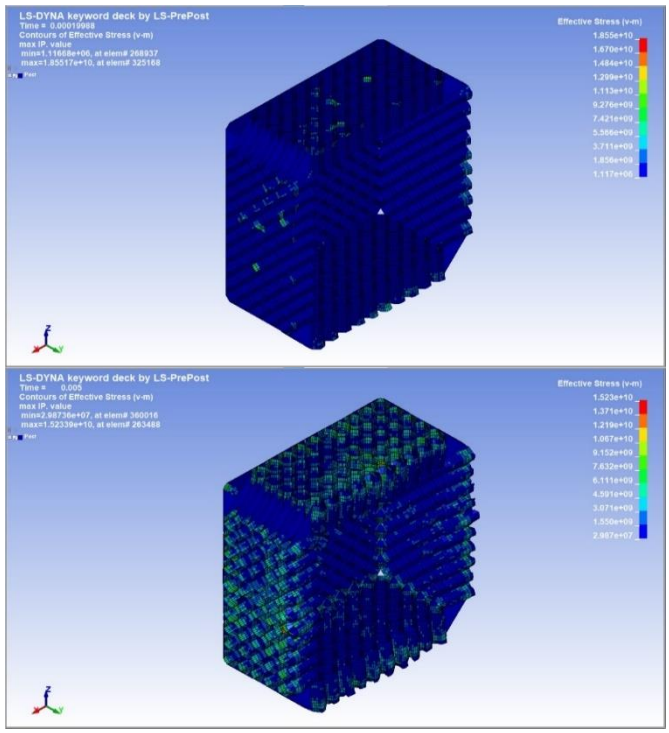

Figure 17. Octagon honeycomb core von-mises stress (first, second, and last phase)

The results of this study demonstrate that increasing the number of sides in the honeycomb core geometry significantly improves the structure's ability to withstand internal blast loads. This finding suggests that optimizing the geometry of honeycomb cores can be an effective design strategy for enhancing the blast resistance of sandwich structures, which could have practical implications for the design of protective systems in industries such as defense, aerospace, and infrastructure. Additionally, the observed relationship between core geometry and blast energy absorption highlights the potential for lightweight, efficient structures that maximize blast mitigation without significantly increasing material costs or weight. In comparing our findings to studies such as Dharmasena et al. [14], who investigated square honeycomb geometries under external blast loading, our study extends the understanding of honeycomb structures by demonstrating that octagonal geometries offer superior blast resistance in internal explosion scenarios. Moreover, the results align with those of Stanczak et al. [15], who noted that increasing the number of honeycomb cells improved blast performance, although our study shows that geometrical changes in individual cells also play a critical role. This comparison highlights how different geometrical configurations, as well as the specific nature of the blast (internal vs. external), impact performance.

One of the unexpected outcomes was the relatively high volatility in the von Mises stress observed in the triangular honeycomb structure compared to the octagonal and square geometries. This finding was initially surprising, as triangular geometries typically provide high structural strength in certain applications. However, upon further reflection, it appears that the internal blast loading results in stress concentrations that are less evenly distributed in geometries with fewer sides, leading to higher stress volatility and more significant deformation. This observation suggests that although triangular configurations are strong in other contexts, they may not be optimal for blast resistance under internal explosions.

5. CONCLUSIONS

Based on the results of the numerical investigation into the response of hollow steel cubes with varying honeycomb core geometries under internal blast loading using LS-DYNA software, the following conclusions can be drawn:

1. The octagonal honeycomb core geometry showed the best performance in resisting blast loads, followed by the square and triangular honeycomb variations. This indicates that increasing the number of sides in the honeycomb core geometry enhances the structure's ability to withstand blast forces.
2. Analysis of von Mises stress data revealed that the octagonal geometry experienced the least volatility in stress, followed by the square and triangular geometries. This lower volatility translates to smaller displacements, reinforcing the observation that geometries with more sides distribute stress more evenly during blast loading.
3. Kinetic energy data showed a direct correlation with displacement, with the octagonal variation exhibiting the least kinetic energy, followed by the square and triangular variations. This indicates that structures with more sides in the core geometry absorb and dissipate blast energy more effectively, resulting in reduced structural displacement and damage.
4. Deformation analysis showed that the triangular honeycomb core geometry resulted in the highest deformation, while the octagonal core had the least deformation, further validating the superior blast resistance of geometries with more sides.
5. Overall, the findings suggest that honeycomb core geometries with a higher number of sides, such as the octagon, offer better blast resistance by reducing displacement, stress, and deformation under internal blast loading. These results contribute to the growing body of knowledge on blast-resistant structures by demonstrating the significance of core geometry in enhancing the performance of honeycomb sandwich structures.

This study advances the understanding of how honeycomb core geometry influences blast resistance, particularly under internal blast conditions—a scenario that has not been extensively studied in prior research. The findings can inform the design of blast-resistant materials and structures, particularly in industries such as defense, aerospace, and civil engineering, where internal blast loads are a significant concern. By optimizing core geometry, engineers can design structures that offer superior protection against blast effects, potentially reducing material failure and improving safety in high-risk environments. However, the study assumed fixed boundary conditions for the back plate and uniform loading across the front plate. Real-world conditions might introduce variabilities in load distribution and constraints, potentially affecting the structural response. The simulations conducted are based on specific geometries and blast intensities; however, further exploration of different geometrical configurations, material types, and loading conditions may be necessary to generalize the findings. Future research could explore further optimization of honeycomb core geometries, including variations in side lengths, cell density, and material composition, to better understand their influence on blast resistance. Additionally, expanding the scope of study to include different blast loading conditions, such as varying explosive sizes, angles of impact, and multi-blast scenarios, could provide deeper insights into the structural performance under more complex conditions. Experimental validation of the numerical results, through physical testing of prototypes, would also be essential for confirming the practical applicability of the findings. Finally, investigating the incorporation of advanced materials, such as composite or functionally graded materials, into the honeycomb core structures could open up new avenues for developing lightweight, high-strength, and highly blast-resistant structures for real-world applications.

REFERENCES

[1] Soleimani, S.M., Ghareeb, N.H., Shaker, N.H. (2018). Modeling, simulation and optimization of steel sandwich panels under blast loading. American Journal of Engineering and Applied Sciences, 11(3): 1130-1140. https://doi.org/10.3844/ajeassp.2018.1130.1140

[2] Wu, C., Lukaszewicz, M., Schebella, K., Antanovskii, L. (2013). Experimental and numerical investigation of confined explosion in a blast chamber. Journal of Loss Prevention in the Process Industries, 26(4): 737-750. https://doi.org/10.1016/j.jlp.2013.02.001

[3] Geretto, C., Yuen, S.C.K., Nurick, G.N. (2015). An experimental study of the effects of degrees of confinement on the response of square mild steel plates subjected to blast loading. International Journal of Impact Engineering, 79: 32-44. https://doi.org/10.1016/j.ijimpeng.2014.08.002

[4] Yao, S., Zhao, N., Jiang, Z., Zhang, D., Lu, F. (2018). Dynamic response of steel box girder under internal blast loading. Advances in Civil Engineering, 2018(1): 9676298. https://doi.org/10.1155/2018/9676298

[5] Baker, W.E., Cox, P.A., Kulesz, R.A., Strehlow, J.J., Westine, P.S. (1984). Explosion Hazards and Evaluation. Elsevier Science Publishers, Amsterdam.

[6] Lu, Y., Xu, K. (2007). Prediction of debris launch velocity of vented concrete structures under internal blast. International Journal of Impact Engineering, 34(11): 1753-1767. https://doi.org/10.1016/j.ijimpeng.2006.09.096

[7] Edri, I., Savir, Z., Feldgun, V.R., Karinski, Y.S., Yankelevsky, D.Z. (2011). On blast pressure analysis due to a partially confined explosion: I. Experimental studies. International Journal of Protective Structures, 2(1): 1-20. https://doi.org/10.1260/2041-4196.2.1.1

[8] Yao, S., Zhang, D., Lu, F., Chen, X., Zhao, P. (2017). A combined experimental and numerical investigation on the scaling laws for steel box structures subjected to internal blast loading. International Journal of Impact Engineering, 102: 36-46. https://doi.org/10.1016/j.ijimpeng.2016.12.003

[9] Li, S., Li, X., Wang, Z., Wu, G., Lu, G., Zhao, L. (2016). Finite element analysis of sandwich panels with stepwise graded aluminum honeycomb cores under blast loading. Composites Part A: Applied Science and Manufacturing, 80: 1-12. https://doi.org/10.1016/j.compositesa.2015.09.025

[10] Zhang, C., Tan, P.J., Yuan, Y. (2022). Confined blast loading of steel plates with and without pre-formed holes. International Journal of Impact Engineering, 163: 104183. https://doi.org/10.1016/j.ijimpeng.2022.104183

[11] Yuan, Y., Zhang, C., Xu, Y. (2021). Influence of standoff distance on the deformation of square steel plates

subjected to internal blast loadings. Thin-Walled Structures, 164: 107914. https://doi.org/10.1016/j.tws.2021.107914
[12] Langdon, G.S., Lee, W.C., Louca, L.A. (2015). The influence of material type on the response of plates to air-blast loading. International Journal of Impact Engineering, 78: 150-160. https://doi.org/10.1016/j.ijimpeng.2014.12.008
[13] Yao, S., Zhang, D., Lu, F. (2016). Dimensionless number for dynamic response analysis of box-shaped structures under internal blast loading. International Journal of Impact Engineering, 98: 13-18. https://doi.org/10.1016/j.ijimpeng.2016.07.005
[14] Dharmasena, K.P., Wadley, H.N., Xue, Z., Hutchinson, J.W. (2008). Mechanical response of metallic honeycomb sandwich panel structures to high-intensity dynamic loading. International Journal of Impact Engineering, 35(9): 1063-1074. https://doi.org/10.1016/j.ijimpeng.2007.06.008
[15] Stanczak, M., Fras, T., Blanc, L., Pawlowski, P., Rusinek, A. (2019). Numerical modelling of honeycomb structure subjected to blast loading. In Proceedings of the 12th European LS-DYNA Conf, Koblenz, Germany, pp. 14-16.
[16] Li, H.J., Shen, C.J., Lu, G., Wang, Z.H. (2022). Response of cylindrical tubes subjected to internal blast loading. Engineering Structures, 272: 115004.
[17] Matsagar, V.A. (2016). Comparative performance of composite sandwich panels and non-composite panels under blast loading. Materials and Structures, 49: 611-629. https://doi.org/10.1617/s11527-015-0523-8
[18] Azzawi, M.M., Hadi, A.S., Abdullah, A.R. (2023). Finite element analysis of crankshaft stress and vibration in internal combustion engines using ANSYS. Mathematical Modelling of Engineering Problems, 10(3): 1011-1016. https://doi.org/10.18280/mmep.100335
[19] Prabowoputra, D.M., Prabowo, A.R., Nubli, H., Harsito, C., Ubaidillah, Susilo, D.D., Wibowo, Lenggana, B.W. (2023). Forecasting effect of blade numbers to cross-flow hydro-type turbine with runner angle 30° using CFD and FDA approach. Mathematical Modelling of Engineering Problems, 10(2): 419-424. https://doi.org/10.18280/mmep.100205
[20] Qin, Y., Yao, X., Wang, Z., Wang, Y. (2022). Experimental investigation on damage features of stiffened cabin structures subjected to internal blast loading. Ocean Engineering, 265: 112639. https://doi.org/10.1016/j.oceaneng.2022.112639
[21] Xu, L., Chen, L., Fang, Q., Dong, Y. (2022). Blast resistance of a folded arch cross-section immersed tunnel subjected to internal explosion. Tunnelling and Underground Space Technology, 125: 104521. https://doi.org/10.1016/j.tust.2022.104521
[22] LS-DYNA Dev, LS-DYNA Theory Manual, vol. 19. ANSYS, Inc. https://ftp.lstc.com/anonymous/outgoing/web/ls-dyna_manuals/DRAFT/DRAFT_Theory.pdf.
[23] Johnson, G.R. (1983). A constitutive model and data for metals subjected to large strains, high strain rates and high temperatures. In Proceedings of the 7th International Symposium on Ballistics, the Hague, Netherlands, pp. 541-547. https://cir.nii.ac.jp/crid/1570854176356644864
[24] Fourney, W.L., Leiste, U., Bonenberger, R., Goodings, D.J. (2005). Mechanism of loading on plates due to explosive detonation. Fragblast, 9(4): 205-217. https://doi.org/10.1080/13855140500431989
[25] Dey, S., Børvik, T., Hopperstad, O.S., Langseth, M. (2007). On the influence of constitutive relation in projectile impact of steel plates. International Journal of Impact Engineering, 34(3): 464-486. https://doi.org/10.1016/j.ijimpeng.2005.10.003.
[26] Alves, M. (2000). Material constitutive law for large strains and strain rates. Journal of Engineering Mechanics, 126(2): 215-218. https://doi.org/10.1061/(ASCE)0733-9399(2000)126:2(215)